

## Elucidation of anti-proliferative and anti-angiogenic potential of novel imidazo[2,1-b][1,3,4] thiadiazole derivatives in Ehrlich ascites tumor model

Ayesha Siddiq<sup>1</sup>, Sadashivamurthy Shamaanth<sup>2</sup>, Mohammed Salman<sup>3</sup>, Dharmappa K. K. <sup>4</sup>, Mantelingu Kempegowda<sup>2</sup>, Shankar Jayarama<sup>5</sup>

<sup>1</sup>Post Graduate Department of Biotechnology, Teresian College, Siddhartha Nagar, Mysore, Karnataka, India

<sup>2</sup>Department of Studies in Chemistry, Manasagangotri, University of Mysore, Mysuru, Karnataka, India

<sup>3</sup>North Medical LLC, (CP) Qiagen, Al Reem Tower, Dafna, Doha, Qatar.

<sup>4</sup>Department of Studies and Research in Biochemistry, Mangalore University, Chikka Aluvara, Somwarpet, Kodagu, Karnataka, India

<sup>5</sup>Department of Studies and Research in Food Technology, Davangere University, Davangere, Karnataka, India-577007

(Received: April 2020

Revised: May 2020

Accepted: June 2020)

Corresponding author: J. Shankar. Email: shankarbio@gmail.com

### ABSTRACT

**Introduction and Aim:** Synthesis of antineoplastic drugs is challenging and shrouded with possibilities of multidrug resistance and numerous side effects. Imidazo[2,1-b] [1,3,4] thiadiazole moieties exhibit tremendous scope as novel anti-cancer molecules. In the present study, we synthesize and characterize a series of 5(a-e) Imidazo [2, 1-b] [1, 3,4]thiadiazole derivatives and evaluate them for antiproliferative properties using *in vivo*, *in vitro*, and *in silico* approach.

**Materials and Methods:** The *in vivo* studies conducted using murine Ehrlich Ascites Cancer (EAC) cell model establishes that treatment with 5c reduces the tumorigenesis by promoting apoptosis in EAC-bearing mice. The cells retrieved from the control and treatment arms of EAC cell bearing mice were used for nuclear and Giemsa staining, DNA fragmentation, RT-PCR and chorioallantoic membrane evaluations.

**Results:** 5c induces apoptosis, plasma membrane degradation, up-regulation of apoptotic genes and anti-angiogenic characteristics. *In vitro* evaluation of 5c using, various cancer cell lines against normal fibroblast 3T3 L1 cells confirm 5c sensitivity to MCF-7 with IC<sub>50</sub> value of 8µM. 5c exudes marked reduction in cell viability, dual nuclear staining, and long-term colony formation assays in these cells.

**Conclusion:** 5c inhibits the growth and proliferation of cancer cells. The results of our molecular docking predictions further substantiate our claim. This study is valuable as 5c exhibits a promising approach for the treatment of cancer and its anti-proliferative potential can be exploited for designing novel anticancer drugs in the near future.

**Keywords:** Imidazo [2,1-b] [1,3,4] thiadiazole derivatives; NMR cytotoxicity, EAC cell; apoptosis; anti-angiogenesis.

### INTRODUCTION

Synthesis of antineoplastic drugs should be done bearing in mind the possibilities of disease reoccurrence (1, 2), multidrug resistance and umpteen side effects of the treating drugs (3-5). At present the future of antineoplastic drug therapy is bleak and shrouded with nebulous challenges of drug contraindications (6, 7).

Imidazo [2,1-b] [1,3,4] thiadiazole moieties exhibit promising anticancer activity. Certain groups (8) have reported that 2, 6-disubstituted imidazo [2,1-b] [1,3,4] thiadiazoles compounds display *in vitro* anticancer activity in tumor cell lines. Others have also demonstrated the anti-proliferative effect of 2-arylimidazo[2,1-b] [1,3,4] thiadiazol-6(5H)-ones 2-phenylimidazo[2,1-b] [1,3,4] thiadiazol-5,6-diones compound (9,10). Structurally in the imidazo[2,1b] [1,3,4] thiadiazole construct, the 1,3,4-thiadiazole moiety functions as a “hydrogen binding domain” while the imidazole nucleus containing compounds are responsible for the biological activities (11).

Synthesis of Imidazo [2,1-b] [1,3,4] thiadiazole moieties exhibit tremendous scope as novel anti-cancer molecules. Taking advantage of its structural scaffold, we have synthesized a unique imidazo-thiadiazole combination series of 2- (4-chlorobenzyl) -5- ((2-substituted- 1H- indol-3-yl) methyl) -6- (4-substituted phenyl) imidazo[2,1-b][1,3,4] thiadiazoles derivatives (5a-e) that were evaluated for their antineoplastic potential. (5a-e) derivatives were characterized through analytical techniques such as LCMS and NMR. The IC<sub>50</sub> values of the chemical constructs were derived using cancerous cell lines such as MCF-7 (breast), HCT-116 (colon) and HeLa (cervical). 5c was selected as the lead compound from the series and thoroughly investigated for its *in vivo*, *in vitro* and *in silico* anti-cancer potential. An Ehrlich ascites carcinoma (EAC) cells, Swiss albino mouse model was developed and *in vivo* anticancer and anti-angiogenic properties of 5c were evaluated in terms of hematology, animal weight and median survival time. Throughout the study, comparisons were drawn to doxorubicin, the standard anticancer

drug. 5c exhibited drastic reduction in tumor growth and neovasculature. Molecular diagnosis and DNA fragmentation of the ascites fluids and histopathology of treated mice helped in elucidating the anti-proliferative potential of 5c. *In vitro* evaluations on MCF-7 cell line ascertained the potential of 5c to induce nuclear aberrations, arrest of colony formation and cell cycle regulation in the cell line. Molecular docking predictions further substantiated our claim about 5c exhibiting strong anti-proliferative potential by up regulation of pro apoptotic genes.

Conclusively we report that our synthesized compound 5c inhibits tumor growth, neovasculature, and increases in lifespan of mice in the EAC mice model. It exhibits antineoplastic potential and causes DNA fragmentation, nuclear lesions and morphological alterations with appearance of apoptotic bodies in the EAC model. Molecular diagnosis of 5c confirms that it up-regulates the expression of pro-apoptotic genes Bax, Caspase 3 and 9 in the MCF-7 cell lines and the EAC mice model. Our study is valuable as 5c exhibits strong anti-proliferative potential mediated through the intrinsic apoptotic pathway, which can be further investigated for designing novel anticancer drugs in the near future.

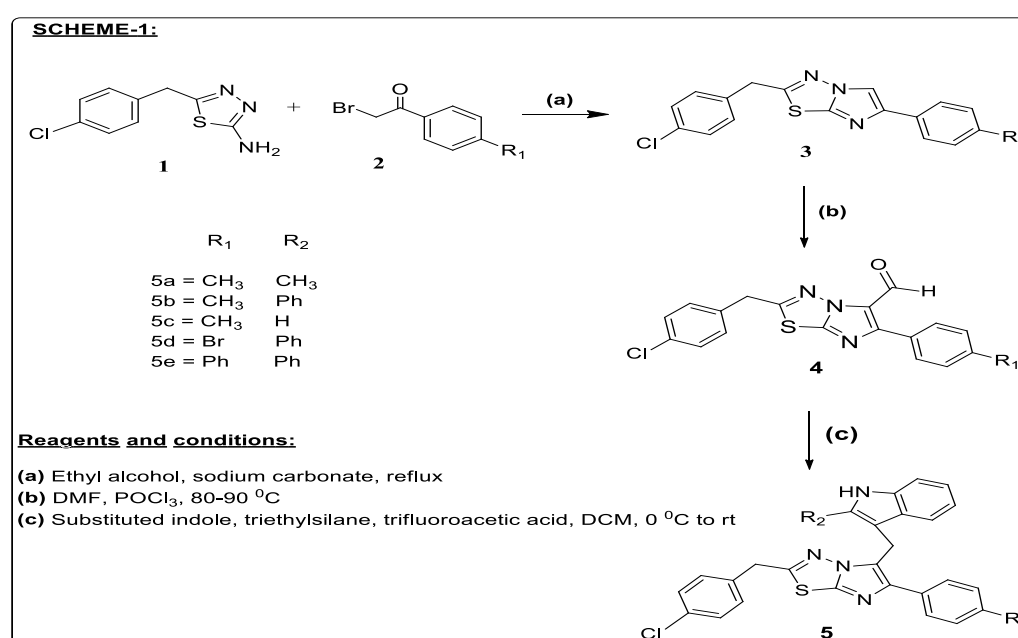
## MATERIALS AND METHODS

Chlorophenyl acetic acid, thiosemicarbazide,  $H_2SO_4$ , phenacyl bromide, ethanol, aqueous sodium carbonate and all the other chemicals involved in the chemical synthesis were procured from Sigma Aldrich. Cell culture mediums and fine chemicals (DMEM, FBS, Trypsin sodium pyruvate, non-essential amino acid, antimyotic antibiotic solution (100X), sodium bicarbonate were purchased from Invitrogen (Carlsbad, CA, USA) or Gibco Life Technologies (St. Louis, MO, USA). Cell lines such as HeLa (cervical cancer), MCF-7 (breast cancer),

HCT-116 (colon cancer) and 3T3 L1 (normal fibroblast) were procured from the National Centre for Cell Science, Pune, India. Cells were grown in appropriate media with 10% heat-inactivated Fetal Bovine Serum (FBS) supplementation, 100U/ml of penicillin and 100 $\mu$ g of streptomycin/ml and incubated at 37°C in a humidified 5% CO<sub>2</sub>. For *in silico* studies, the three dimensional structure of anti apoptotic proteins were retrieved from RCSB protein data bank. Docking studies of 3D structure of anti apoptotic proteins were performed using AutoDock version 4.2.3. Lamarckian genetic algorithm (LGA) was used for docking as discussed later.

### Synthesis of Imidazo [2,1-b] [1,3,4] thiadiazole derivatives 5(a-e)

The starting material 5- (4-chlorobenzyl) -1,3,4-thiadiazol-2-amine (1) was prepared from 4 chlorophenylacetic acid and thiosemicarbazide using  $H_2SO_4$  as solvent at 75°C for 6hrs. 2(4-chlorobenzyl)-6- (4-substituted phenyl)- imidazo [2,1-b] [1,3,4] thiadiazole derivatives (3a-3c) were prepared by refluxing 5-(4-chlorobenzyl)- 1,3,4- thiadiazol- 2- amine (1) with the appropriate phenacyl bromide (2) in ethanol for 8hrs, and quenching with aqueous sodium carbonate. The various phenacyl bromides (2a-2c) were bought from Sigma-Aldrich, USA. 2-(4-chlorobenzyl) -6- (4-substituted phenyl) imidazo[2,1-b][1,3,4] thiadiazole-5-carbaldehydes (4a-4c) were prepared by using VilsmeierHaack condition ( $POCl_3$  and DMF) on the corresponding 2- (4-chlorobenzyl)-6- (4-substitutedphenyl)- imidazo [2,1-b] [1,3,4] thiadiazole (12-14). 2- (4-chlorobenzyl) -5- ((2- substituted- 1H-indol-3-yl) methyl) -6- (4-substituted phenyl) imidazo [2,1-b] [1,3,4] thiadiazole (5a-5e) were prepared by treating corresponding aldehydes (4a-4c) and 2-substituted indoles in presence of triethylsilane hydride and trifluoroacetic acid in DCM at 0-5°C. (Scheme 1).



**Scheme 1:** Synthesis of Imidazo[2,1-b] [1,3,4] thiadiazole derivatives 5(a-e)

**In Vivo****Animals and care**

Male Swiss albino mice 6 to 8 weeks and around 25-28g were used. They were provided standard rearing condition (12:12-hour light/dark cycles, 50%  $\pm$  5% humidity and temperature of 25 $\pm$ 2°C) and housed in cage. Pellet diet was *ad libitum* with free access to water. All the animal investigations were permitted by the Institutional Animal Ethics Committee (IAEC), (Approval No: BCP/IAEC/EXTP/04/2018) Bharathi College of Pharmacy, Bharathi Nagara, Mandya District, India. The experiments were carried in agreement with the Committee for the purpose of control and supervision of experiments on animals (CPCSEA) guidelines for laboratory animal facility.

**Scheme**

Ehrlich ascites carcinoma (EAC) cells are malignant cells with a short lifespan and grow rapidly seventh day onwards of intraperitoneal implantation into the mice peritoneal cavity. EAC cell mice model usually survive for approximately 16-20 days after cancer implantations (through i.p routes). Tumor growth was evaluated in terms of increase in ascites cell volume and neovascularization of blood vessels (proliferation and angiogenesis). In this study, we used doxorubicin (2 mg/kg b.wt) as the positive control and 5c (20 mg/kg b.wt) as the treatment arm. Both were administered i.p on the 7, 9, and 11<sup>th</sup> day after the tumor cell transplantation. Cell viability was ascertained through trypan blue exclusion assay.

**Experimental layout**

30 male Swiss albino mice were distributed into 3 groups:

Group I- EAC-bearing mice + Saline (1 ml /kg b.wt)  
 Group II – EAC-bearing mice + 5c (20 mg/kg b.wt)  
 Group III – EAC-bearing mice + Doxorubicin (2 mg/kg b.wt). Tumor end points were measured for changes in the hematology, animal weight, changes in ascites fluid volume, median survival time (MST), angiogenesis, histopathology and percentage increase in the lifespan of the animal (% ILS)

%ILS=MST of treatment arm-MST of control arm / MST of control group $\times$ 100

ILS score of 25% or above that of control was categorized as good anti-tumor response.

**Acridine orange/ethidium bromide staining**

Since we hypothesized that our compound 5c was anti-proliferative and could induce DNA lesions to cancerous cells, we stained the nucleus with acridine orange and ethidium bromide procedure (AO/EtBr) as described earlier (15). Briefly  $1\times 10^6$  EAC cells were collected from both the control and treatment groups of 5c. Cells were smeared on glass slides and fixed in 3:1 ratio of methanol: acetic acid. Thereafter they were hydrated with PBS, stained with (AO/EtBr) (1:1) and then washed with PBS to be

viewed under a fluorescent microscope at a wavelength of 500nm (16).

**DNA fragmentation**

Ascites cells from control and EAC arms were analyzed for DNA fragmentation following previous published protocol (17). Briefly, DNA isolates were run on an agarose gel and photographed under gel dock.

**Giemsa staining**

Analysis of induction of apoptotic bodies was done by following previous protocol (18, 19). Briefly, EAC cells smears were air dried and fixed in methanol: acetic acid solution (3:1). Subsequently PBS washes were given after which smear was stained with 0.1% Giemsa solution and photographed under a light microscope.

**RT-PCR**

Semi quantitative reverse transcriptase polymerase chain reaction (RT-PCR) analysis of the genes involved was done following previous protocol (20). Total RNA was extracted from both control and treatment groups of EAC cells and estimated through Trizol method (Invitrogen). In short, 1 $\mu$ g of RNA from each sample was used for cDNA synthesis using reverse transcriptase cDNA synthesis kit (Applied Biosystems). Using specific primers, relative expression of transcripts for all genes (Bax, Bcl-2 Caspase 3, and Caspase 9) were ascertained using SYBR Green chemistry. GAPDH was taken as an internal control.

**Peritoneal angiogenesis and Chorioallantoic membrane assay (CAM)**

This was performed in accordance to the protocol (21, 22) - to access the anti-antigenic effect of 5c. Briefly, 5c was evaluated for its ability to inhibit angiogenesis and microvasculature from the internal covering of the peritoneal pit in euthanized animals. Recombinant vascular endothelial growth factor (rVEGF165) induced CAM angiogenesis in fertilized egg approach was also performed and alterations in vascularization pattern were studied.

**IN VITRO SCREENING****MTT**

We screened 5(a-e) for *in vitro* anti-proliferative potential by employing various cell lines such as HeLa (cervical cancer), MCF-7 (breast cancer), and HCT-116 (colon cancer). These were selected as many cancer deaths occurring both in males and females were reported to be arising from these origins (23). For cytotoxicity and cell viability evaluation, HeLa (cervical cancer), MCF-7 (breast cancer), HCT-116 (colon cancer) and normal fibroblastic cell lines 3T3 L1 were seeded at a density of  $1\times 10^6$  cells/well in a 96-well plate and grown in standard conditions (37°C with 5% CO<sub>2</sub>)

for 24hrs and further exposed to increasing concentrations of synthesized compounds 5(a-e) ranging from 6.25 $\mu$ M to 200 $\mu$ M. Synthesized compounds were referred as treatment group and dissolved in DMSO, while the vehicle group were given DMSO alone. After 24hrs of exposure, cells were treated with MTT (5mg/ml) for 4hrs. Insoluble formazan crystals that were formed in the process were further treated with 50 $\mu$ l of DMSO and the absorbance was read at a wavelength 560 nm (24, 25, and 26).

#### Nuclear staining - (AO/EtBr)

In this study, we used doxorubicin as the positive control (1.75 $\mu$ M) and 5c as the treatment arm (7 $\mu$ M and 14 $\mu$ M). Briefly, 1 $\times$ 10<sup>6</sup> MCF-7 cells were harvested from both vehicle and treatment groups and nuclear staining was performed as mentioned earlier (27).

#### Clonogenic assay

To study the complete effect of our synthesized compound we performed long-term colony formation assays for 10 days using previously published protocol with slight modifications (20). 1,000 cells were seeded on a 12-well plate followed by addition of 5c (7 $\mu$ M & 14 $\mu$ M) and doxorubicin as the positive control (1.75 $\mu$ M), the next day. Cells were fixed with 10% formalin and incubated at 37°C for 10 days and stained with crystal violet (0.05% solution) for 30min. Images were taken with a flatbed scanner after thorough washing of the plates. For quantification, 1ml methanol was added to each well to extract the dye and absorbance measured at 540nm.

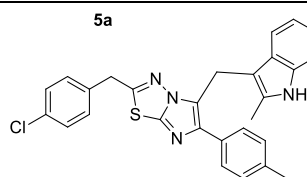
#### Quantitative Determination of Apoptosis by Flow Cytometry

Since compound 5c inhibited the cell proliferation, its effect on cell cycle progression was analyzed. Briefly, 1 $\times$ 10<sup>6</sup> MCF-7 cells were harvested from both vehicle and treatment groups and nuclear DNA dual labeling with Annexin V: FITC and propidium iodide (PI) were performed according to manufacturer's protocol (Becton Dickinson) and analyzed by flow cytometry (Becton Dickinson) (25). The cells, which were Annexin V: FITC positive and PI negative were identified as early apoptotic, while Annexin V: FITC and PI positive as late apoptotic.

#### IN SILICO

#### Protein preparation

**Table 1:** Structure and yield of Imidazo[2,1-b] [1,3,4] thiadiazole derivatives 5(a-e)

Compound Name	Structure of Compound	Molecular Weight	% of isolated yield
2-(4-chlorobenzyl)-5-((2-methyl-1H-indol-3-yl)methyl)-6-(p-tolyl)imidazo[2,1-b][1,3,4]thiadiazole	 <p>5a</p>	483.0270	52

The three-dimensional structures of and Bcl-2 and Bcl-XL anti apoptotic proteins with PDB id 1R2D and 2O2F were retrieved from RCSB protein data bank. For docking stimulation, the hetero atoms of 1R2D was removed and hydrogen atoms was added. Further, gasteiger charges was computed and saved into PDBQT file using Auto Dock tool version 4.2.3 (28).

#### Ligand preparation

The ligands 5c (2-(4-chlorobenzyl)-5-((2-methyl-1H-indol-3-yl)methyl)-6-(p-tolyl)imidazo[2,1-b][1,3,4]thiadiazole) was detected with 24 aromatic carbon and 5 rotatable bonds. For the ligand, the torsion was put at 5 and charges added that was saved in a PDBQT format (29).

#### Molecular docking of 5c with Bcl-2 and Bcl-XL

Docking studies of 3D structures of anti-apoptotic proteins with PDB id 1R2D and 2O2F with ligand 5a was performed using AutoDock version 4.2.3. A grid map was prepared using AutoGrid with XYZ of 60  $\times$  60  $\times$  60 Å with spacing of 0.525 Å and grid center dimension X, Y and Z was 18.594, -0.002 and 71.171 Å respectively. Lamarckian genetic algorithm (LGA) was used for docking with 150 set as the population size and other parameters were kept as default. The maximum number of energy evaluation and maximum number of generations was set to 2500000 and 27000 respectively (29).

## RESULTS

#### Design and Chemistry

Structural verification of all compounds synthesized was done by various spectral techniques such as <sup>1</sup>H NMR, <sup>13</sup>C NMR, and mass analysis. All compounds that were synthesized displayed a good correlation in the spectral and analytical data to the proposed structures. <sup>1</sup>H-NMR spectra of 5c had all the peaks at expected positions along with proper number of protons. Methyl protons were found at  $\delta$  2.262 as singlet. Two benzyl peaks were observed at  $\delta$  4.405 and 4.449 with two protons each as singlet. Thirteen aromatic protons were observed between  $\delta$  6.883 and 7.604. One -NH- proton resonates at  $\delta$  10.820 as singlet. The corresponding compound yields in the scheme are listed in Tables 1 and 2. The detailed spectral data and spectra of all the synthesized compounds and intermediates have been provided as supplementary material.

2-(4-chlorobenzyl)-5-((2-phenyl-1 <i>H</i> -indol-3-yl)methyl)-6-( <i>p</i> -tolyl)imidazo[2,1- <i>b</i> ][1,3,4]thiadiazole		545.0964	55
5-((1 <i>H</i> -indol-3-yl)methyl)-2-(4-chlorobenzyl)-6-( <i>p</i> -tolyl)imidazo[2,1- <i>b</i> ][1,3,4]thiadiazole		469.0004	65
6-(4-bromophenyl)-2-(4-chlorobenzyl)-5-((2-phenyl-1 <i>H</i> -indol-3-yl)methyl)imidazo[2,1- <i>b</i> ][1,3,4]thiadiazole		609.9659	65
2-(4-chlorobenzyl)-6-phenyl-5-((2-phenyl-1 <i>H</i> -indol-3-yl)methyl)imidazo[2,1- <i>b</i> ][1,3,4]thiadiazole		531.0698	65

## IN VIVO

### Effect of 5c on EAC mice model

5c was injected intraperitoneally at a dose of 20 mg/kg b.wt into the peritoneal cavity of EAC bearing mice. The results of our study show that, compound 5c decreased the mice body weight from the treatment group as compared to the control group (Fig 1A). The percentage survival time for mice treated with 5c was increase (28/29 days) as compared to the control group (17/18 days) (Fig 1B). Further 5c also decreased the ascites volume 2-fold as compared to control group indicating that compound 5c actively suppressed the tumor volume in treatment arm (Fig 1C). We also observed that compound 5c decreased the ascites cell number by

66% as against 78% for doxorubicin (20 mg/kg b.wt) when compared to control (Fig. 1D). A decrease in the organ weight and hematological profile of treatment arms was observed. Furthermore, we also evaluated the morphological changes in the appearance of tissues obtained from different organs (liver, spleen and kidney) through H&E staining. Results of our study showed that liver sections reported mild hepatocytic degeneration with mild fatty changes and fibrosis, spleen had normal splenic sinusoids and lymphoid architecture and kidney showed normal renal architecture with occasional hemorrhagic and mild inflammatory changes as against normal control for each organ (Fig. 1E-F-G: supplementary material).

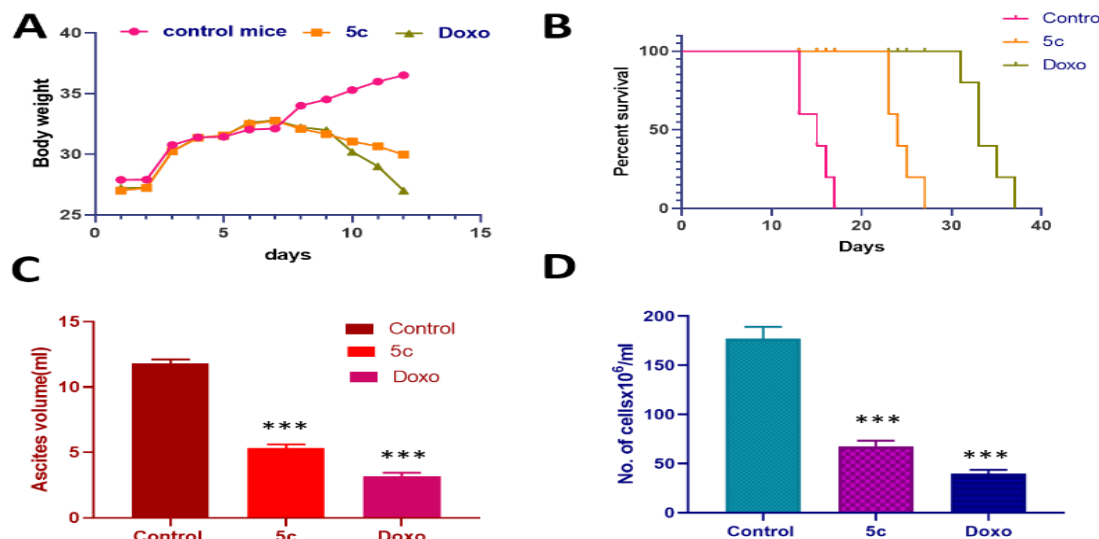


**Fig. 1:** 5c exhibits, anti-proliferative potential in EAC bearing mice model **A:** Decreased body weight of EAC tumor-bearing mice. **B:** The Gehan-Breslow-Wilcoxon test graph curve displays the comprehensive survivability of 5c treated mice. **C:** Reduced levels in ascites fluid discharge. **D:** Decline in the number of tumor cells. Data are presented as Mean  $\pm$  S.E.M. N=10. Statistically significant values are (\*P < 0.05, \*\*P < 0.01; \*\*\*P < 0.001).

### Analysis of nuclear lesions, morphological alterations and DNA lesions

Ascites cells from EAC groups of both 5c and control were nuclear stained with acridine orange/ ethidium bromide (AO/EtBr). Our results indicated that 5c showed significantly greater apoptosis as evident by the uptake of EtBr fluorescence to completely orange-yellow color (Fig. 2A-C). Using Giemsa

stain, we further evaluated the potential of 5c to cause induction of apoptosis in terms of morphology changes as plasma membrane degradation, formation of apoptotic bodies and shrinkage of cells (Fig. 2D-F). Ascites cells from EAC groups that were analyzed for induction of DNA lesions also showed fragmentation of DNA in the 5c treatment arm (Fig. 2G).

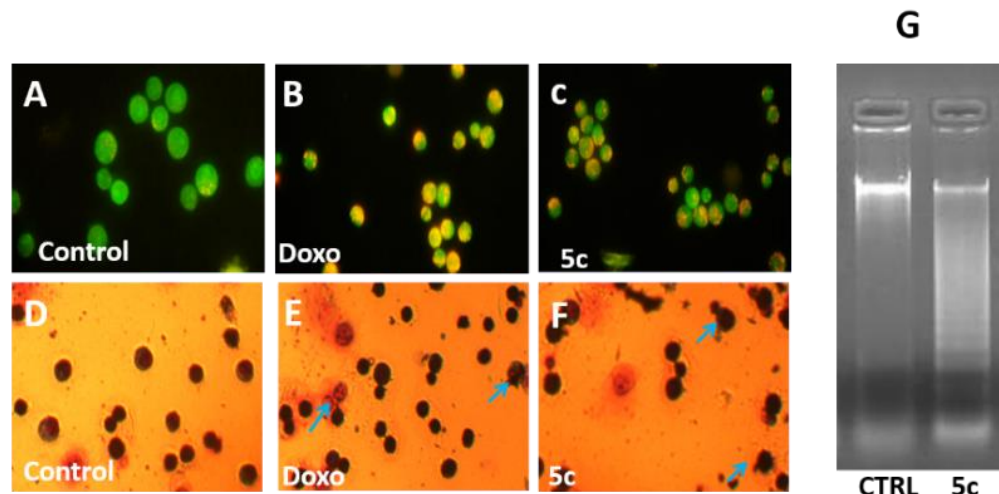


**Fig. 2:** 5c encourages Apoptosis of Ehrlich Ascites Carcinoma cells. Pro-apoptotic effect of 5c is examined by nuclear staining methods and DNA fragmentation assay. **Fig. 2A-C:** explains AO/EtBr staining and **Fig. 2D-F**, illustrate Giemsa staining. **G:** 5c shows nuclear DNA fragmentation in Ehrlich Ascites Carcinoma cells.

### Expression of apoptotic genes of ascites cell

The results of our study showed that sample 5c showed higher index of anti-proliferative potential in terms of induction of apoptosis in the ascites cells extracted from EAC groups of both 5c and control group (Fig. 3A). There was marked dose dependent increase in relative expression levels of Bax with 5c showing 2-fold and positive control, doxorubicin showing 2.2-fold increase in expression levels as

compared to control (Fig. 3C). 5c also showed increase in expression levels of both Caspase 9 and 3 genes. For Caspase 9, the increase was between 1.1-1.2-fold for both 5c and doxorubicin and for Caspase 3 it was 1.1-1.3-fold higher for 5c and doxorubicin as compared to control (Fig. 3B). For Bcl-2 there was a decrease in the expression levels of both 5c and doxorubicin: 2.2-2.4-fold as compared to control (Fig. 3C).

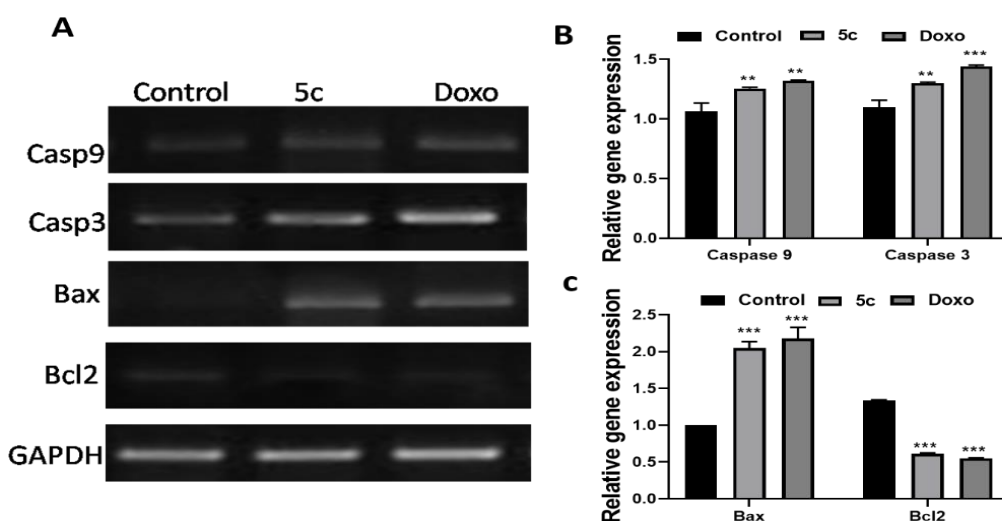


**Fig. 3:** *In-vivo* gene expression of Caspase 9, Caspase 3, Bax and Bcl-2 by semi quantitative RT-PCR (Reverse Transcriptase-Polymerase Chain Reaction) of 5c on Ascites fluid cell retrieved from euthanized mice from treatment and control arm.

Data are presented as Mean  $\pm$  S.E.M. (\*P < 0.05, \*\* P < 0.01; \*\*\* P < 0.001).

Cas 9: Lanes: 1=control; 2=5c (20mg); 3=Doxorubicin (2mg).

Cas 3: Lanes: 1=control; 2=5c (20mg); 3=Doxorubicin (2mg).

Bax: Lanes: 1=control; 2=5c (20mg); 3=Doxorubicin (2mg).

Bcl2: Lanes: 1=control; 2=5c (20mg); 3=Doxorubicin (2mg).

GAPDH: Lanes: 1=control; 2=5c (20mg); 3=Doxorubicin (2mg).

### Peritoneal angiogenesis and in ova chorioallantoic membrane assay (CAM)

This was performed to access the anti-angiogenic effect of 5c as it is a cardinal feature in cancer diagnosis. After treatment with 5c we observed for features of intraperitoneal angiogenesis in treated mice. The results of our study showed that, 5c treatment showed a significant reduction in the formation of blood vessel as compared to control mice. Further, VEGF secretion in ascites fluid was also determined by the ELISA plate method. Our results showed that, VEGF secretion was significantly decreased in 5c arm as compared to

control mice. Recombinant vascular endothelial growth factor (rVEGF<sub>165</sub>) induced CAM angiogenesis in fertilized egg approach was also performed and alterations in vascularization pattern were studied. The anti-angiogenic effect of 5c was also evaluated through rVEGF<sub>165</sub> induced in vivo CAM assay and we observed that 5c strongly inhibited formation of the new blood vessel in developing embryos. It was noteworthy to record the responses obtained for 5c treatment arm were comparable to doxorubicin that was used as a positive control (Fig. 4 A-B).

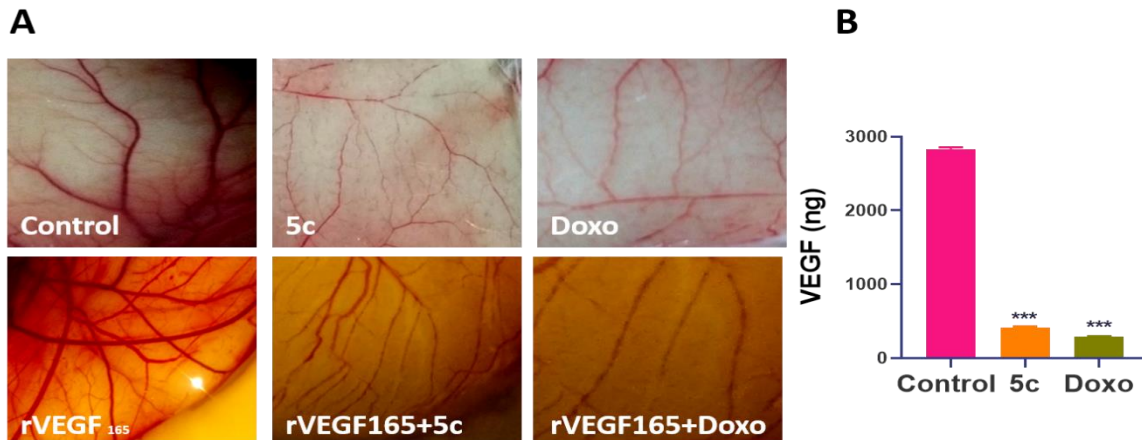


**Fig. 4:** 5c exhibits anti-angiogenic effect as seen in In vivo CAM pictures presenting the reduced range of rVEGF165-induced angiogenesis.

### IN VITRO

#### MTT assay

Compounds of series 5(a-e) were screened *in vitro* for their anti-proliferative properties against various cell lines such as HeLa (cervical cancer), MCF7

(breast cancer) and HCT-116 (colon cancer). The results of our study showed that 5c affected the viability of cancer cells over human fibroblast normal cells in a dose and time dependent manner (Fig. 5; Table 2).

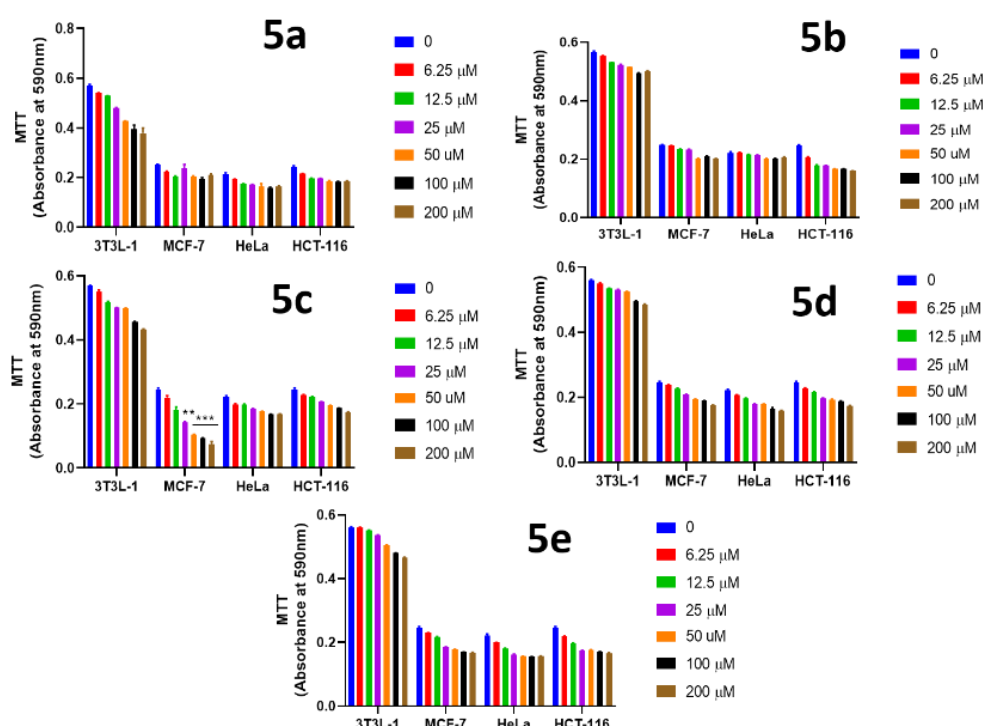


**Fig. 5:** *In-vitro* screening of synthesized compounds for their cytotoxicity. Effects of 5a, 5b, 5c, 5d, and 5e on 3T3-L1, MCF-7, HeLa and HCT-116 cell lines by MTT assay. Data are presented as Mean  $\pm$  S.E.M. (\*P < 0.05, \*\* P < 0.01; \*\*\* P < 0.001).

### Dual staining

Our hypothesis was that the imidazo derivative was antiproliferative and could induce DNA lesions to MCF-7 cells; compound 5c was nuclear stained with acridine orange/ ethidium bromide (AO/EtBr). Our

results indicated that 5c showed significantly greater apoptosis as evident by the uptake of EtBr fluorescence to completely orange-yellow color in a dose dependent manner at 7 $\mu$ M and 14 $\mu$ M concentrations (Fig. 6A-D).

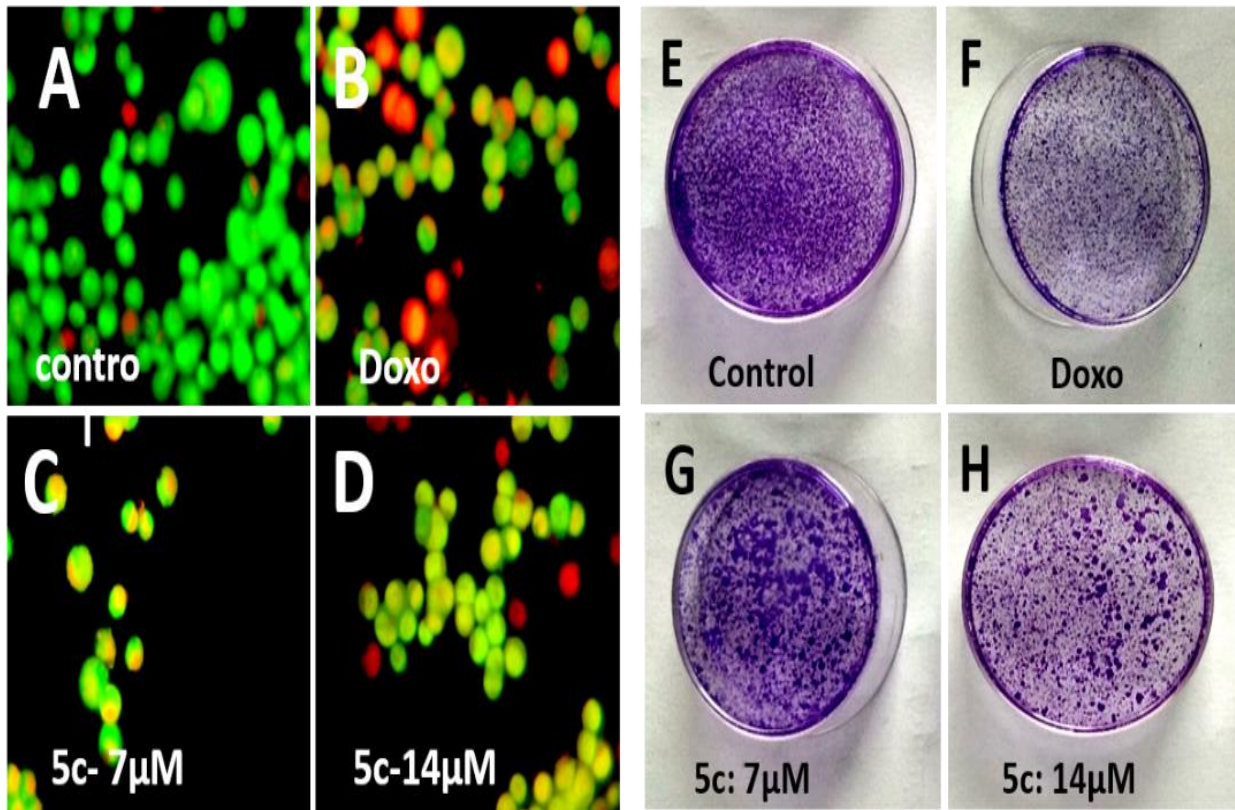


**Fig. 6A-D:** *In-vitro* cytotoxic evaluation of dual staining for 5c through Acridine Orange and Ethidium Bromide (AO/EtBr) on MCF-7 cell line. **Fig. 6E-H:** *In-vitro* cytotoxic evaluation of 5c for colony formation assay on MCF-7 cell line.

### Clonogenic assay

The MCF-7 cells treated with compounds 5c showed inhibition of colony formation as compared to the control. Our results showed that their surviving fraction (%) were 100 for control, 48.66 and 44.36 for 7 $\mu$ M and 14 $\mu$ M for compound 5c respectively.

Cells treated at 14 $\mu$ M of compound 5c showed significant inhibition in colony formation in comparison to other treated cells which show approximately minimal inhibition relative to control. Overall 5c at 14 $\mu$ M showed comparatively better inhibition of colony formation (Fig. 6E-H; Table 3).

**Table 2:** IC<sub>50</sub> of derivatives 5(a-e) on MCF-7, HeLa, HCT-116

Cell lines	IC <sub>50</sub> in $\mu$ M				
	5a	5b	5c	5d	5e
MCF-7	43.37 $\pm$ 0.03	65 $\pm$ 0.12	8 $\pm$ 0.09	70 $\pm$ 0.07	60.6 $\pm$ 0.04
HeLa	72.54 $\pm$ 0.02	97.18 $\pm$ 0.06	127 $\pm$ 0.04	127.8 $\pm$ 0.08	120.1 $\pm$ 0.12
HCT-116	71.02 $\pm$ 0.12	142.5 $\pm$ 0.02	191.7 $\pm$ 0.07	101.4 $\pm$ 0.04	12.3 $\pm$ 0.09

**Table 3:** Table indicating the colony count of control and treated cells at different concentrations on MCF-7 cell line

Sample name	Conc. $\mu$ M	Colony count	Plating efficiency %	Surviving fraction %
Control	0	2085	41.7	100.00
5c	7	1136	22.72	48.66
	14	925	18.5	44.36

### Quantitative determination of apoptosis by flow cytometry

The results of our study showed that 5c induced a significant proportion of cells to undergo apoptosis, as determined by the flow cytometric analysis. Dot plot results showed that in the early phase of

apoptosis as compared to control, (positive control) doxorubicin showed 3-fold increase and lower and higher doses of 5c showed dose independent fold increase (2.2-3.2-fold). Again, in the late phase of apoptosis (Fig. 7A-E) doxorubicin was 4-fold increased and 5c (3.5-4.25-fold).

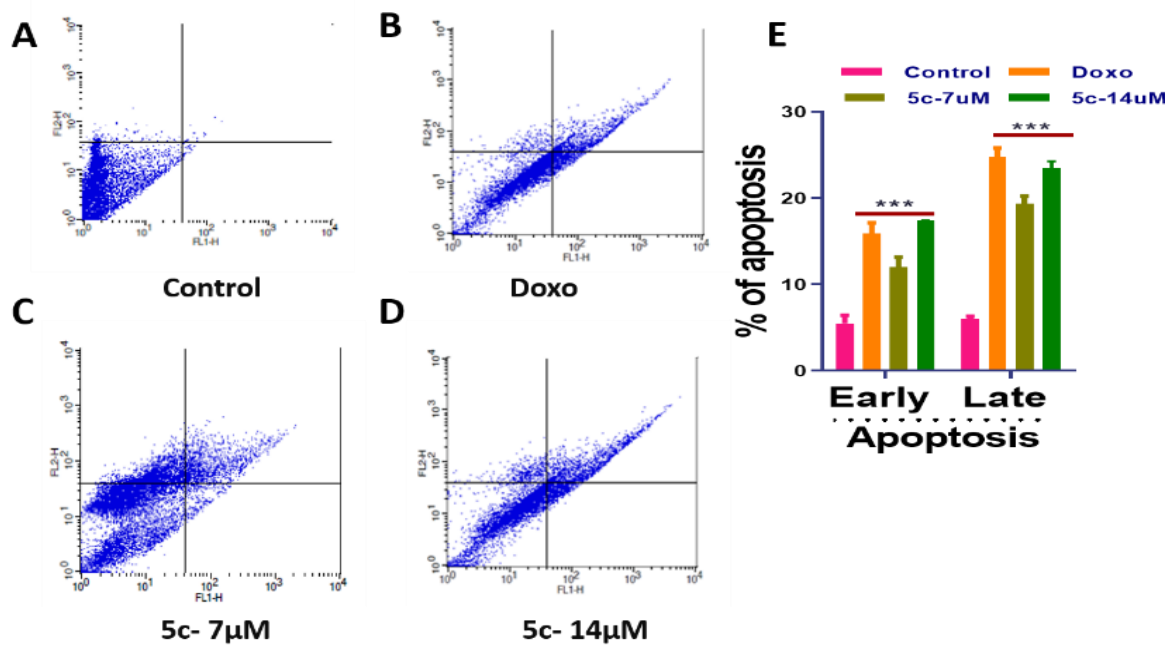


**Fig. 7:** Detection of apoptosis induced by 5c in MCF-7 cell lines. After treatments 5c (7 and 14 $\mu$ M) for 48hrs, MCF-7 cells were stained with Annexin V-FITC and PI, and analyzed by flow cytometry. (A) Control (B) Doxorubicin (1.75 $\mu$ M) 5c (C-D: 7 and 14 $\mu$ M) (E) percentage of cells in different apoptotic phases. In each panel, the lower right quadrants represent early apoptotic cells. The upper right quadrants contain late stage apoptotic cells. Data are presented as Mean  $\pm$  S.E.M. where (\*P < 0.05, \*\*P < 0.01; \*\*\*P < 0.001).

### In silico studies

Analysis of the docking results showed higher binding affinity of 5c ligand with 1R2D protein with binding energy of -7.02 kcal/mol respectively. 5c ligand formed one hydrogen bond with TYR101 of 1R2D protein with a bond length of 2.07 Å. Further, the aromatics rings of the 5c ligand formed  $\pi$ - $\pi$  interaction with PHE 105 of 1R2D protein and positively charge amide group of ARG132 exhibited cation-  $\pi$  interaction. In our studies, we found that Tyr101, Phe105, ASN136, ARG100 and ARG 132 were major contributors to binding. BH3-binding hydrophobic groove of 1R2D was characterized by the residues such as Ala 93, Phe 97, Ala 104, Phe 105, Leu 108, Val 126, Leu 130, Ala 142, Phe 146, Lys 138, and Glu 96 with reference to binding of natural peptides such as Bad and Bak. Present docking analysis also validated the active site as

being composed of mentioned residues such as Phe 105, Leu 108, Phe 97, Leu 130, Ala 142, Gly 138. Also coherent with previous mutational studies involving Gly 138, Tyr 101, Arg 139, and Leu 130 formed interaction with the above said residues. Therefore, the observed best hits 5c may have potential to act as competitive inhibitors of protein, rendering the binding site inaccessible to natural substrates. Docking studies of 3D structure of anti-apoptotic protein with PDB id 2O2F were ranked. Analysis of the docking results showed the higher binding affinity of 5c ligand with 2O2F protein with binding energies of -8.93 kcal/mol. 5c ligand formed one hydrogen bond with GLY142 of 2O2F protein with a bond length of 2.223 Å. Furthermore, the aromatics rings of the 5c ligand formed  $\pi$ - $\pi$  interaction with PHE 101 and TYR105 of 2O2F protein (Fig 8A-B)

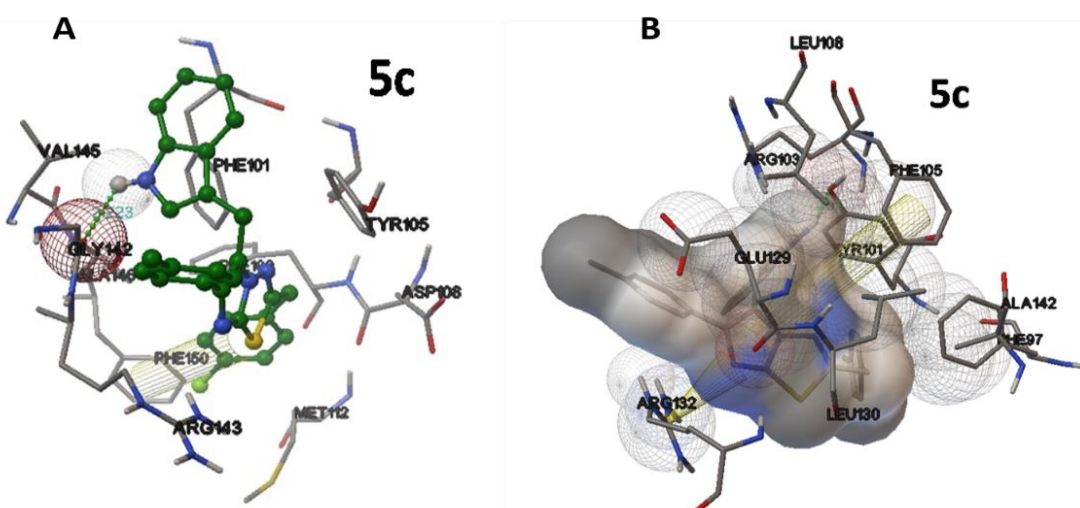


**Fig. 8:** Compound 5c was docked with the binding pocket of anti-apoptotic protein Bcl-2 (Fig. 8A) and Bcl-XL (Fig. 8B).

**Table 4:** Interaction results between ligands and receptors

Ligand	Target protein	Binding Energy (kJ mol <sup>-1</sup> )	Ligand Efficiency	Inhibition Constant (μM)	vdW+H-bond + desolv energy	No. H-bonds	'ligand' - 'receptor close
5c	2O2F(Bcl-2)	-8.93 kcal/mol	-0.27	284.3	-10.35	1 bond GLY142 bond length -> 2.223	VAL145, MET112, GLY142, ARG143, ASP108, TYR 105, PHE109, PHE 101, ALA 146, PHE150
5c	1R2D(Bcl-XL)	-7.02 kcal/mol	-0.21	7.12	-8.4	1 bond TYR101 bond length - 2.07	PHE105, LEU130, LEU108, ARG103, PHE97, GLU129, ALA142, TYR101, ARG132

## DISCUSSION

As anti-apoptosis is one of the major parameter responsible for the birth of cancer, targeting apoptosis and its genes responsible is of greater interest. It is reported in the earlier studies that the imidazothiadiazole moiety downregulate the anti-apoptotic protein Bcl-2 and upregulates Pro-apoptotic proteins such as Bax, Bid. Therefore, we synthesized a series of derivatives of imidazothiadiazole moiety to study their impact on cancer. Among the series of compounds screened, 5c successfully inhibited the effect of EAC cells. It caused a dose dependent regression on the body weight of mice, decreased the ascites volume and cell number (as a direct affect) and increased the MST of treatment arm as against control mice. 5c was nontoxic as evident from the results of H&E staining of various organs as compared to their respective control groups. An ideal anticancer agent should reinstall the apoptotic machinery within cancer cells and our results conclusively state that 5c displayed successful induction of apoptosis as characterized by the induction of nuclear lesions, morphological blebblings, irregular shapes and induction of apoptotic bodies in the ascites cells. Moreover, 5c was also able to induce fragmentation of DNA within the ascites cells. Compound 5c has an apoptosis enhancing capability in the ascites cells extracted from EAC groups of both 5c and control group. 5c modulates the anti and pro-apoptotic gene regulation through intrinsic pathways of apoptosis. The apoptotic response exhibited by 5c on the ascites cells further suggests the efficacy and possible application of our compound in cancer prevention and therapy. Apoptosis is crucial in cancer progression. A major strategy in chemotherapy is to cause cell death through induction of apoptotic machinery in the targeted tumor cells. Likewise, our compound 5c was able to up regulate the expression levels of pro apoptotic genes as Bax, Caspase 3 and 9 and down regulate the expression level of anti-apoptotic gene Bcl-2 and thus was able to sensitize the cancerous cells to apoptotic mode of cell death,

thus fulfilling the antineoplastic criteria. Angiogenesis is a cardinal hallmark of tumor growth and our compound 5c displayed strong anti-angiogenic potential by inhibiting neovascularization in both peritoneal cavity and the ovum thus qualifying as a suitable antineoplastic agent. 5c exhibited maximum cytotoxic activity on MCF-7 cell line with the IC<sub>50</sub> value 8μM respectively, which may be due to the presence of methyl substitution on phenyl ring attached to imidazole moiety. The compounds 5a, 5b, 5d and 5e have shown IC<sub>50</sub> values around 43-70μM in all the three cell lines might be due to the presence of bulky phenyl group on indole. It can be concluded that, electron-donating groups like methyl have shown more cytotoxic activity in our compounds when compared to electron withdrawing groups like chloro or bromo. Therefore, 5c and 5a were taken as lead compounds along with MCF-7 as a cell line of choice. The lower and higher concentrations of 5c that were considered for further investigations were (7 and 14) μM. Annexin V-FITC/PI double staining was performed to study the mechanism of action of 5c mediated tumor inhibition in MCF-7 cell line. The fact that, 5c shows comparability in fold increase to doxorubicin qualifies it to be contested as an anti-neoplastic agent. The designed small molecules function as inhibitors of anti-apoptotic Bcl-2protein (Bcl-2). B-cell lymphoma-2 anti-apoptotic proteins (Bcl-2, Bcl-XL, Bcl-w,) prevent apoptosis either by sequestering proforms of death-driving cysteine proteases (a complex called the apoptosome) or by averting the release of mitochondrial apoptogenic factors such as cytochrome c and AIF (apoptosis-inducing factor) into the cytoplasm. Hence, we hypothesized that designing of selective inhibitors of the Bcl-2proteins seems to be the most promising strategy to "cut-short" pro-survival pathways and commit the cancer cells to apoptosis by permeabilizing the outer membrane of the mitochondrion. Thus considering the pro-apoptotic properties of Imidazo[2,1-b][1,3,4]thiadiazole moiety, we performed comparative molecular docking studies of 5c with Bcl-2 and Bcl-XL to clarify the binding mode of the

compounds and to evaluate their antiproliferative potential.

## CONCLUSION

Our *in vivo* and *in vitro* studies reveal that our synthesized compounds Imidazo[2,1-b] [1,3,4] thiadiazole derivative 5c shows strong anti-proliferative, anti-angiogenic potential. It successfully induced apoptosis in the ascites cells through the upregulation of pro-apoptotic genes. It also caused nuclear lesions, DNA fragmentation and morphological alterations as blebbing in both the ascites and MCF-7 cells. 5c strongly inhibited neovasculature in tumor cells and thus qualifies strongly as a potent anticancer drug. These results are further substantiated from the data received from the docking scores, which gives an accurate understanding of ligand and receptor binding interaction, in our case 5c Bcl-2 and Bcl-XL. This study is valuable as 5c exhibits a promising approach for the treatment of cancer and its antiproliferative potential can be exploited for designing novel anticancer drugs in the near future. Moreover, further studies on molecular levels are required to validate the study which can answer the targeted mechanism of 5-((1*H*-indol-3-yl)methyl)-2-(4-chlorobenzyl)-6-(*p*-tolyl)imidazo[2,1-b][1,3,4]thiadiazole as an anti-cancer agent. The compound can also be researched on inflammation which is a factor caused by cancer.

## ACKNOWLEDGEMENT

AS thank The Directorate of Minorities fellowship, Government of Karnataka for financial support (DOM/Fellowship CR-62/2017-18).

**CONFLICT OF INTEREST:** The authors report no conflict of interest.

## REFERENCES

1. Ferlay, J., Colombet, M., Soerjomataram, I., Mathers, C., Parkin, D. M., Piñeros, M., *et al.* Estimating the global cancer incidence and mortality in 2018: GLOBOCAN sources and methods. *International Journal of Cancer*. 2019 Apr 15; 144(8): 1941-1953.
2. Wong, M. C., Goggins, W. B., Wang, H. H., Fung, F. D., Leung, C., Wong, S. Y., *et al.* Global incidence and mortality for prostate cancer: analysis of temporal patterns and trends in 36 countries. *European Urology*. 2016 Nov 1; 70(5): 862-874.
3. Brown, K. F., Rungay, H., Dunlop, C., Ryan, M., Quartly, F., Cox, A., *et al.* The fraction of cancer attributable to modifiable risk factors in England, Wales, Scotland, Northern Ireland, and the United Kingdom in 2015. *British Journal of Cancer*. 2018 Apr; 118(8): 1130-1141.
4. Islami, F., Goding Sauer, A., Miller, K. D., Siegel, R. L., Fedewa, S. A., Jacobs, E. J., *et al.* Proportion and number of cancer cases and deaths attributable to potentially modifiable risk factors in the United States. *CA: A Cancer Journal for Clinicians*. 2018 Jan; 68(1): 31-54.
5. Wilson, L. F., Antonsson, A., Green, A. C., Jordan, S. J., Kendall, B. J., Nagle, C. M., *et al.* How many cancer cases and deaths are potentially preventable? Estimates for Australia in 2013. *International Journal of Cancer*. 2018 Feb 15; 142(4): 691-701.
6. Lingaraju, G. S., Balaji, K. S., Jayarama, S., Anil, S. M., Kiran, K. R., Sadashiva, M. P. Synthesis of new coumarin tethered isoxazolines as potential anticancer agents. *Bioorganic & Medicinal Chemistry Letters*. 2018 Dec 15; 28(23-24): 3606-3612.
7. Miyahara, M., Kamiya, S., Nakadate, M., Sueyoshi, S., Tanno, M. Antitumor effect of compounds synthesized in the Division of Synthetic Chemistry (VI). *Eisei Shikenjo hokoku. Bulletin of National Institute of Hygienic Sciences*. 1982; 100: 163-165.
8. Noolvi, M. N., Patel, H. M., Kamboj, S., Kaur, A., Mann, V. 2, 6-Disubstituted imidazo [2, 1-b][1, 3, 4] thiadiazoles: Search for anticancer agents. *European Journal of Medicinal Chemistry*. 2012 Oct 1; 56: 56-69.
9. Taher, A. T., Georgey, H. H., El-Subbagh, H. I. Novel 1, 3, 4-heterodiazole analogues: Synthesis and in-vitro antitumor activity. *European Journal of Medicinal Chemistry*. 2012 Jan 1; 47: 445-451.
10. Karki, S. S., Panjamurthy, K., Kumar, S., Nambiar, M., Ramareddy, S. A., Chiruvella, K. K., *et al.* Synthesis and biological evaluation of novel 2-aryl-5-substituted-6-(4'-fluorophenyl)-imidazo [2, 1-b][1, 3, 4] thiadiazole derivatives as potent anticancer agents. *European Journal of Medicinal Chemistry*. 2011 Jun 1; 46(6): 2109-2116.
11. Terzioglu, N., Gürsoy, A. Synthesis and anticancer evaluation of some new hydrazone derivatives of 2, 6-dimethylimidazo [2,1-b][1,3,4]thiadiazole-5-carbohydrazide. *European Journal of Medicinal Chemistry*. 2003 Jul 1; 38(7-8): 781-786.
12. Iyer, D., Vartak, S. V., Mishra, A., Goldsmith, G., Kumar, S., Srivastava, M., *et al.* Identification of a novel Bcl-2-specific inhibitor that binds predominantly to the BH1 domain. *The FEBS Journal*. 2016 Sep 1; 283(18): 3408-3437.
13. Jain, A. K., Sharma, S., Vaidya, A., Ravichandran, V., Agrawal, R. K. 1, 3, 4-Thiadiazole and its derivatives: A review on recent progress in biological activities. *Chemical Biology & Drug Design*. 2013 May; 81(5): 557-576.
14. Bandgar, B. P., Patil, S. A., Korbad, B. L., Biradar, S. C., Nile, S. N., Khobragade, C. N., *et al.* Synthesis and biological evaluation of a novel series of 2, 2-bisaminomethylated aurone analogues as anti-inflammatory and antimicrobial agents. *European Journal of Medicinal Chemistry*. 2010 Jul 1; 45(7): 3223-3227.
15. Srinivas, G., Anto, R. J., Srinivas, P., Vidhyalakshmi, S., Senan, V. P., Karunagaran, D. Emodin induces apoptosis of human cervical cancer cells through poly (ADP-ribose) polymerase cleavage and activation of caspase-9. *European Journal of Pharmacology*. 2003 Jul 25; 473(2-3): 117-125.
16. Gao, X., Zhang, X., Hu, J., Xu, X., Zuo, Y., Wang, Y., *et al.* Aconitine induces apoptosis in H9c2 cardiac cells via mitochondria-mediated pathway. *Molecular Medicine Reports*. 2018 Jan 1; 17(1): 284-292.
17. Devegowda, P. S., Balaji, K. S., Prasanna, D. S., Swaroop, T. R., Kameshwar, V. H., Jayarama, S., *et al.* Synthesis, characterization of 4-anilino-6, 7-dimethoxy quinazoline derivatives as potential anti-angiogenic agents. *Anti-Cancer Agents in Medicinal Chemistry (Formerly Current Medicinal Chemistry-Anti-Cancer Agents)*. 2017 Dec 1; 17(14): 1931-1941.
18. Mahassni, S. H., Al-Reemi, R. M. Apoptosis and necrosis of human breast cancer cells by an aqueous extract of garden cress (*Lepidium sativum*) seeds. *Saudi Journal of Biological Sciences*. 2013 Apr 1; 20(2): 131-139.
19. Shivaprakash, P., Balaji, K. S., Lakshmi, G. M., Chandrashekara, K. T., Jayarama, S. Methanol extract of *Caesalpinia bonducuella* induces apoptosis via up-regulation of Bax and activation of PARP in Ehrlich Ascites tumor cells. *Med Aromat Plants*. 2016; 5: 2167-0412.
20. NA, F., Rodermond, H. M., Stap, J., Haveman, J., van Bree, C. Clonogenic assay of cells *in vitro*. *Nature Protocols*. 2006; 1(5): 2315-2319.

21. Balaji, K. S., Priyanka, S., Preethi, S. D., Chandrashekara, K. T., Lokesh, S., Rangappa, K. S. Angio-suppressive effect of Clitoria Ternatea flower extracts is mediated by HIF-1 $\alpha$  and down-regulation of VEGF in Murine carcinoma model. *Med Chem.* 2016; 6(7): 515-520.
22. Chen, W., Zheng, R., Zeng, H., Zhang, S., He, J. Annual report on status of cancer in China, 2011. *Chinese Journal of Cancer Research.* 2015 Feb; 27(1): 2.
23. Devegowda, P. S., Balaji, K. S., Prasanna, D. S., Swaroop, T. R., Jayarama, S., Siddalingaiah, L., *et al.* Pro-apoptotic activity of novel 4-anilinoquinazoline derivatives mediated by up-regulation of bax and activation of poly (ADP-ribose) phosphatase in ehrlich ascites carcinoma cells. *Asian Journal of Chemistry.* 2017 Apr 1; 29(4): 896.
24. Roopashree, R., Mohan, C. D., Swaroop, T. R., Jagadish, S., Raghava, B., Balaji, K. S., *et al.* Novel synthetic bisbenzimidazole that targets angiogenesis in Ehrlich ascites carcinoma bearing mice. *Bioorganic & Medicinal Chemistry Letters.* 2015 Jun 15; 25(12): 2589-2593.
25. Rakesh, K. S., Jagadish, S., Balaji, K. S., Zameer, F., Swaroop, T. R., Mohan, C. D., *et al.* 3, 5-Disubstituted isoxazole derivatives: Potential inhibitors of inflammation and cancer. *Inflammation.* 2016 Feb 1; 39(1): 269-280.
26. Petros, A. M., Nettesheim, D. G., Wang, Y., Olejniczak, E. T., Meadows, R. P., Mack, J., *et al.* Rationale for Bcl-xL/Bad peptide complex formation from structure, mutagenesis, and biophysical studies. *Protein Science.* 2000 Dec; 9(12): 2528-2534.
27. Sattler, M., Liang, H., Nettesheim, D., Meadows, R. P., Harlan, J. E., Eberstadt, M., *et al.* Structure of Bcl-xL-Bak peptide complex: recognition between regulators of apoptosis. *Science.* 1997 Feb 14; 275(5302): 983-986.
28. Lu, H. F., Sue, C. C., Yu, C. S., Chen, S. C., Chen, G. W., Chung, J. G. Diallyl disulfide (DADS) induced apoptosis undergo caspase-3 activity in human bladder cancer T24 cells. *Food and Chemical Toxicology.* 2004 Oct 1; 42(10): 1543-1552.
29. Iyer, D., Vartak, S. V., Mishra, A., Goldsmith, G., Kumar, S., Srivastava, M., *et al.* Identification of a novel Bcl-2-specific inhibitor that binds predominantly to the BH1 domain. *The FEBS Journal.* 2016 Sep 1; 283(18): 3408-3437.